

# Characterization of 3D-Printed Choke Horn Antenna for 5G Backhaul Applications.

Carlos Biurrun-Quel<sup>1</sup>, Elsa Lacombe<sup>2,3</sup>, Frederic Giancesello<sup>2</sup>, Cyril Luxey<sup>3</sup>, Carlos Del-Río<sup>1,4</sup>

<sup>1</sup> Department of Electrical, Electronic and Communication Engineering, Universidad Pública de Navarra, Spain.

[carlos.biurrun@unavarra.es](mailto:carlos.biurrun@unavarra.es)

<sup>2</sup>STMicroelectronics, 38920 Crolles, France. [elsa.lacombe@st.com](mailto:elsa.lacombe@st.com), [frederic.giancesello@st.com](mailto:frederic.giancesello@st.com)

<sup>3</sup>Polytech'Lab, Université Nice Sophia Antipolis, 06560 Valbonne, France. [cyril.luxey@unice.fr](mailto:cyril.luxey@unice.fr)

<sup>4</sup>Institute of Smart Cities (ISC), Universidad Pública de Navarra, Spain. [carlos@unavarra.es](mailto:carlos@unavarra.es)

**Abstract**— The 200 and 320 GHz frequency band constitutes an interesting window with approximately constant attenuation, which could potentially have applications in the area of ultra-high-capacity wireless links. The user's demand of data for future 5G mobile systems will require backhaul systems to be able to provide several dozens of GHz in order to satisfy those demands. Furthermore, additive manufacturing techniques stand as an interesting way of reducing costs without sacrificing performance. In this work, a choke horn antenna, designed at a central frequency of 240 GHz and manufactured by 3D-printing technology is presented. This antenna is thought to serve as the feed of a compact parabolic reflector. The antenna has been measured by Near- and Far-Field techniques and these measurements show an adequate agreement with simulation results. Additionally, the measurement set-up included a novel dynamic time-domain, software-controlled gating that readjusts itself for every measured point.

**Index Terms**—Additive manufacturing, choke horn, measurement, dynamic time-domain gating, , backhaul.

## I. INTRODUCTION

The upper part of the mmWave band, 200-320 GHz, also considered as the lower part of the Terahertz region, offers an interesting opportunity for high speed radio links, providing more than 100 GHz bandwidth with reasonably constant atmospheric losses [1]. In order to provide enough capacity to the final user in future 5G communication systems for which 1 Gbps is expected, a required throughput of several tens of gigabits shall be demanded at the access points. Thinking of backhaul radio links, this is translated into a bandwidth of dozens of GHz, depending on the modulation that would be implemented, its spectral efficiency and the Signal to Noise Ratio available at the receiver.

However, the use of this band entails some limitations. First of all, one of the main handicaps nowadays at these frequencies is power generation and design of amplifying equipment, which requires achieving a trade-off between great bandwidth operation, low noise temperature and significant gain. In addition, in order to increase the performance of the radio links, the requirements for antenna design include the use of highly directive antennas, ~50 dBi, so as to compensate the large amount of propagation loss and

atmospheric attenuation in the link. This could be achieved by employing reflector antennas.

A well-known relationship is established between the gain of an aperture antenna and the surface of its aperture. As seen in Equations 1 and 2, an approximated value of the diameter (D) of the reflector dish can be obtained for a desired gain value (G). With this formula, determining an approximated value for the diameter of the required reflector dish is straight-forward. Assuming a conservative value for the aperture efficiency,  $e_a=0.5$ , and an operational frequency of 240 GHz, the diameter of a 50-dBi antenna would result in a value of around 18 cm.

$$A_{eff}/G = e_a \cdot A_{phy}/G = \lambda^2/4\pi \quad (1)$$

$$A_{phy} = \pi \cdot r^2 = \pi \cdot (D/2)^2 (G \cdot \lambda^2) / (4\pi \cdot e_a) \quad (2)$$

One illustrative parameter of reflector antennas is the relation between its focal length and the diameter (f/D). This is a geometrical relation that can easily be formulated in terms of the subtended angle between the focus and the edge of the reflector dish ( $\theta_0$ ), see Eq. 3 (reformulated from Eq. 15-25 in [2]). Fig. 1 sketches the geometry of a parabola. Typically, a normalised value of -10dB is desired at the edge of the dish in order to achieve a balance between the illuminated area and the radiation spillover. In the case of a 12 dBi feed-horn, this value is obtained approximately at  $\theta_0=40^\circ$ , throwing a value of 0.7 for the f/D relation. From this relation, the focal length can be extracted directly, being around 12.5 cm in this case. These values could be reduced even further by increasing the aperture efficiency.

$$f/D = 1 / (4 \cdot \tan(\theta_0/2)) \quad (3)$$

Up-to this point, it has been ascertained that reflector antennas stand as compact, highly directive solutions for high-capacity communication links in the lower region of the Terahertz band.

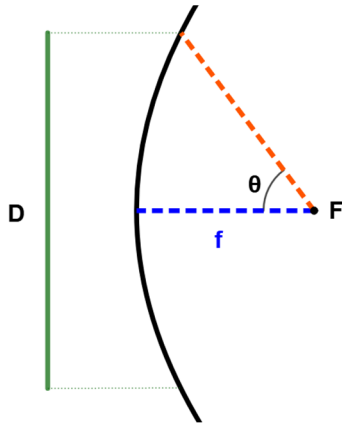


Fig. 1. Geometry of a parabola.

In this paper, a choke horn antenna fabricated by means of additive manufacturing techniques is presented. These technologies are increasingly becoming more popular for fabricating millimetre-wave components [3], including the space segment [4]. Authors in [5] validated this technology by presenting a novel plastic lens fabricated by additive manufacturing at 240 GHz. A remarkable work was recently presented [6] and comprises the design and measurement of a corrugated horn operating between 1.25 and 1.57 THz, manufactured by means of direct machining. However, no approaches have been found, to the best knowledge of the authors of this work, in the fabrication and measurement of horn antennas at the targeted frequency band.

The fabrication of the antenna was commissioned to SWISSto12 [7]. It was manufactured by means of stereolithography and then metallized.

Subsequently, it was received and measured at our own laboratory. The measuring campaign consisted on two different procedures, Far-Field and Planar Near-Field, which are later compared among themselves and the simulated results, after applying a Near-Field to Far-Field transformation (NF2FF) [8], [9] to the Near-Field measurements. This antenna could be thought to serve as a feedhorn in a parabolic reflector system, although no implementation in such a system is yet presented in this work.

The aim of this contribution is to demonstrate the feasibility of using additive manufacturing technology for horn antennas above 200 GHz and also to prove the capability of measuring antennas at these frequencies, rather than presenting a novel feedhorn design. The design of the horn antenna is presented in the section II of this paper. Then, the measurement campaign is explained and the results are discussed. By last, some conclusions are drawn.

## II. DESIGN OF THE HORN ANTENNA

The presented antenna is a choke horn, designed to have a 12 dBi gain over the 200 GHz to 280 GHz bandwidth. Table I summarizes the main features and dimensions of the horn. Its length is 7.22 mm, however, it includes a 2.8 mm-thick UG-387/U flange with standard holes for subsection with alignment pins and screws, making the overall length slightly higher than 10 mm.

TABLE I. MAIN ANTENNA FEATURES

Dimension	Value
Total antenna length (L)	10.22 mm
Total antenna aperture (A)	4.06 mm
Number of chokes	3
Thickness of chokes (w)	0.3 mm
Number of steps in transition	3
Gain at boresight	12 dBi

A caption of the 3D simulated half-model is shown in Fig. 2, where the cross-section is also presented. It includes a rectangular, WR4.3 standard to circular waveguide transition, in order to allow direct connection with standard waveguide components. This transition has been inserted inside the flange and stands as one of the most challenging parts of the horn, from the manufacturing perspective.

## III. MEASUREMENTS

As previously introduced, two different procedures have been followed: Planar Near-Field and Far-Field measurements. The experimental set-up for the measurement techniques is shown in Fig. 3. The same set-up was used for both measures, given the possibility to control each axis separately. X and Y axis were used for the planar Near-Field measurement, together with roll axis  $\theta_1$  and  $\theta_2$ , which were used for obtaining the E- and H-Planes. As for the Far-Field measurement, only  $\phi_1$  and the aforementioned  $\theta_1$  and  $\theta_2$  were used in order to obtain the different cuts of interest.

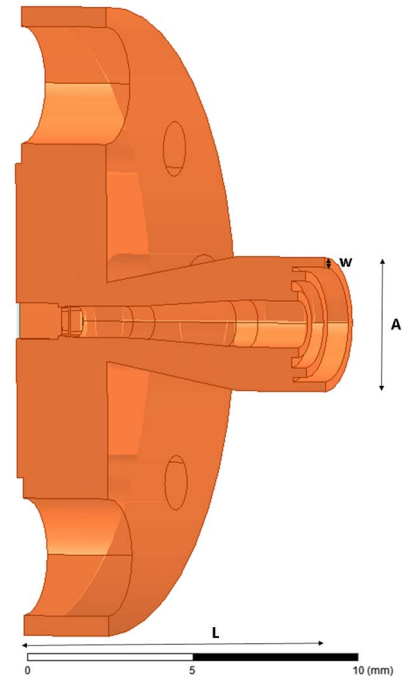


Fig. 2. 3D-(Half)Model of the 240 GHz horn antenna.

As for the equipment used in the measurement campaign, an Agilent PNA-X N5242A Vector Analyser (26.5 GHz) and two VDI external mixers, for the 220-340 GHz frequency band in WR3.4 standard waveguide, were used. It is important to remark that the output of the mixers was given in WR3.4 standard waveguide, while the input waveguide of the AUT (Antenna Under Test) was given in WR4.3. This mismatch in the waveguide dimensions might have caused an additional insertion loss. However, the dynamic range of the measurement set-up was wide enough to assume this extra loss without affecting the reliability of the results. Fig. 4 shows the manufactured antenna, AUT, screwed to one of the mixers.

In both cases, a time gating technique was used to isolate the arriving pulse, avoiding scattered contributions that were assumed to be generated by reflections in the surroundings of the set-up such as screws, flanges, and other possible scatterers. While in the Far-Field scenario the time-domain gating was fixed (since the turn centre is fixed, the distance from the AUT to the probe remains constant), in the case of the Near-Field scenario, the time gate was adjusted dynamically, in order to correct the distance between the probe and the AUT at each sampling point in the measured plane. This has been made by configuring the span of the gating at the central position of the plane, assuring that the main pulse is included in the gating. This span is maintained during the whole measuring process, while its central position is shifted for each measured point, taking into account the distance to this point from the central position. At this central point the distance is minimal and at any other point it becomes larger. This increase in the distance is translated into a shift in the time of reception. The whole process is controlled by software, thus no human intervention is needed, except for previous calibration and fixing of the gating span.

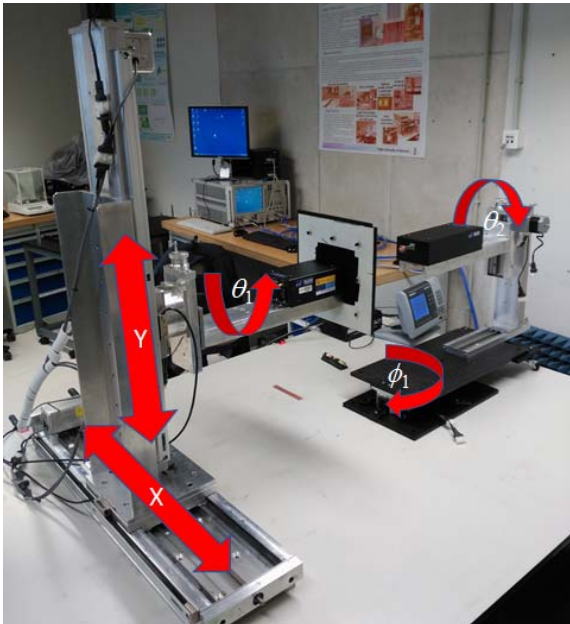


Fig. 3. Picture of the Measurement set-up.

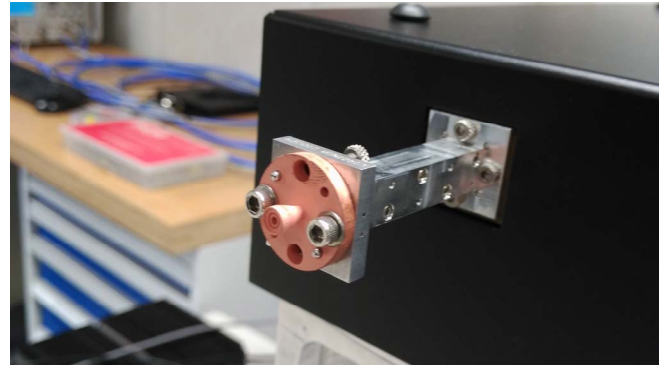


Fig. 4. Picture of the Manufactured horn antenna (AUT), screwed to one of the external VDI mixers.

For the planar Near-Field antenna measurement, an 8x8cm plane at a distance of 4 cm was chosen in order to guarantee at least -30 dB difference between the measured E-field at the central point of the plane and at its edges. The Near-Field to Far-Field transformation (NF2FF) was performed offline. For this purpose, magnitude and phase of the electric field were previously measured and stored. The effect of the measuring probe [9], that otherwise would alter the measured fields, was also corrected through an offline processing.

The measured points preserved a sampling span of  $\lambda/2$  between each other in order to prevent from creating aliasing after applying the transformation. This implemented feature resulted of great importance in the measuring process, since the plane swept was considerably big in terms of wavelengths ( $64\lambda \times 64\lambda$  for the central frequency of interest), making the measurement process extremely time-consuming.

Fig. 5 shows the simulated and measured (in both far- and near-field techniques) radiation pattern of the antenna at 240 GHz for both E- and H-Planes. Dotted lines correspond to the simulation results while solid lines represent the measured ones. Red and light green lines correspond to the E-plane in Far- and Near-Field, respectively, while blue and pink lines correspond to their counterparts in the H-plane. The measured results show reasonable agreement with simulation results. Some ripples at the NF2FF radiation pattern can be observed. These are thought to be caused by two main reasons.

First of all, parasitic reflection from other elements were included in the time-domain gating, despite the dynamic gate. Specifically, the screws that hold the antenna, whose size was comparable to the size of the antenna and whose position was not far enough to be excluded by the time-domain gating, were observed to alter the measured fields of the antenna. Secondly, the measuring process itself, which limits the measured area to a defined plane and involves a truncation error. For this reason, a spatial window effect aliasing is created after applying the transformation and results not contained in the interval  $\theta \in [-55^\circ, 55^\circ]$  are excluded due to lack of reliability.

#### ACKNOWLEDGMENT (*Heading 5*)

This work has been supported by Spanish Ministry of Economy, Industry and Competitiveness, PCIN-2016-073 in the framework of European CHIST-ERA project Call 2015, TERALINKS.

#### REFERENCES

- [1] F. Al-Ogaili and R. M. Shubair, "Millimeter-wave mobile communications for 5G: Challenges and opportunities," 2016 IEEE International Symposium on Antennas and Propagation (APSURSI), Fajardo, 2016, pp. 1003-1004
- [2] C. A. Balanis, *Antenna Theory - Analysis and Design*, 3rd ed. Hoboken, New Jersey: John Wiley & Sons, 2005.
- [3] J.P. Anderson, J.L. Doane, A. Haid, and N. Alexander, in 2016 41st Int. Conf. Infrared, Millimeter, Terahertz Waves (IEEE, 2016), pp. 1–2.
- [4] J. Teniente, J.C. Iriarte, R. Caballero, D. Valcazar, M. Goni, and A. Martinez, *IEEE Antennas Wirel. Propag. Lett.* 1 (2018).
- [5] E. Lacombe, F. Gianesello, A. Bisognin, C. Luxey, D. Titz, H. Gulan, T. Zwick, J. Costa, and C.A. Fernandes, in *2017 IEEE Int. Symp. Antennas Propag. Usn. Natl. Radio Sci. Meet.* (IEEE, 2017), pp. 5–6.
- [6] A. Gonzalez, K. Kaneko, and S. Asayama, "1.25–1.57 THz Dual-Polarization Receiver Optics Based on Corrugated Horns," *IEEE Trans. Terahertz Sci. Technol.*, vol. 8, no. 3, pp. 321–328, May 2018.
- [7] Swissto12.com (2018). Swissto12. [Online] Available at: <http://www.swissto12.com/>. [Accessed 10 Apr. 2018].
- [8] A. Yaghjian, "An overview of near-field antenna measurements," in *IEEE Transactions on Antennas and Propagation*, vol. 34, no. 1, pp. 30-45, Jan 1986
- [9] C. Taybi, M. A. Moutaouekkil, K. K. Rodrigues, B. Elmagroud and A. Ziyyat, "Probes correction for planar near field antennas measurements," 2015 IEEE 15th Mediterranean Microwave Symposium (MMS), Lecce, 2015, pp. 1-4.

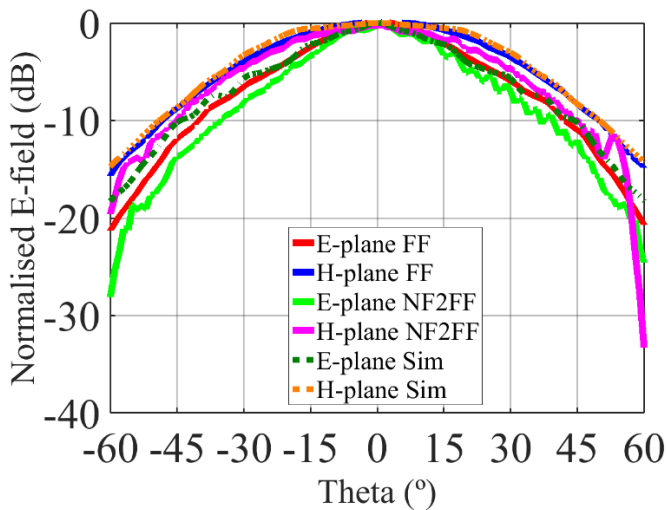


Fig. 5. Simulated and measured radiation pattern of the antenna at 240 GHz.

Possible manufacturing errors could also be responsible for this disagreement. However, it can be observed that Far-Field measurements show great agreement with simulated results. For this reason, it seems feasible to discard that hypothesis and assert that the additively-manufactured horn fulfils the expected performance. All in all, it could be concluded that the measurement technique hereby presented is suitable for measuring mmWave horns above 200 GHz (from 200 to 280 GHz).

#### IV. CONCLUSIONS

In this paper, a 12dBi choke antenna designed at 240 GHz and manufactured by 3D-printing technology has been presented. This antenna would be capable of working as a feed-horn in a compact-sized, single-parabolic reflector configuration, for high-capacity backhaul links in future 5G systems.

Measurements of the radiation patterns of the AUT have been performed using both Far- and planar Near-Field techniques. Near-field measured data has been later processed offline in order to apply the NF2FF transform and to correct the effect of the measuring probe. A dynamic time-domain gating has been applied in order to prevent the measuring process from being affected by undesired reflections, especially those observed at the edges of the plane. However, it was observed that the metallic screws, used to attach the antenna to the mixer through their flanges, coupled part of this radiation and thus altered the measure pattern. Dielectric screws shall be used in order to solve this issue. Nevertheless, the measured patterns were generally observed in good agreement with simulation results.

Therefore, an example of the feasibility of using additive manufacturing technology for high-frequency (above 200 GHz), mmWave horn antennas has been provided. These techniques allow a reduction in manufacturing and prototyping costs and their used shall be encouraged in future works. Simultaneously, this work provides an example of the feasibility to measure antennas at these high frequencies with reasonable accuracy.